Hindawi
Modelling and Simulation in Engineering
Volume 2024, Article ID 6500007, 17 pages
https://doi.org/10.1155/2024/6500007

Research Article

Modeling and Simulation of the Effect of Airbag Thickness on the Performance of Extended Handle Pneumatic Floor Jack

Abduljebar Mahmud Aliy,[1] **Ramesh Babu Nallamothu**,[2] **and Abdulbasit Nasir**[3]

[1]*Department of Vehicles and Machinery Maintenance, Ethiopian Construction Works Corporation, P.O. Box 21952/1000, Addis Ababa, Ethiopia*
[2]*Department of Mechanical Engineering, School of Mechanical Chemical and Materials Engineering, Adama Science and Technology University, P.O. Box 1888, Adama, Ethiopia*
[3]*Department of Mechanical Engineering, Faculty of Manufacturing, Institute of Technology, Hawassa University, P.O. Box 5, Hawassa, Ethiopia*

Correspondence should be addressed to Ramesh Babu Nallamothu; ramesh.babu@astu.edu.et

Received 25 January 2024; Revised 25 March 2024; Accepted 30 March 2024; Published 25 April 2024

Academic Editor: Rahul Pandey

In the process of changing tires, drivers require a suitable lifting device, namely, a jack, that can be inserted into a designated slot strategically positioned beneath the vehicle. Similarly, in workshops and maintenance facilities, jacks are essential for part replacements and maintenance. This research focuses on the design and analysis of extended handle pneumatic floor jacks specifically tailored for light-duty vehicles. The aim is to enhance effectiveness by enabling the repair of multiple vehicles simultaneously using a single compressor. The study utilizes ANSYS 2022R1 to assess the structural weaknesses of pneumatic airbags, aiming to explore technological advancements and develop an optimal airbag design capable of lifting light vehicles. Natural rubber is utilized as the airbag material, with thicknesses of 2.5 mm, 2.75 mm, and 3 mm. The study investigates three different airbag behaviors: von Mises stress, strain, and deformation in two directions. A pressure of 8.2 MPa is applied, and a weight of 4000 kg is imposed. The results indicate that the 2.5 mm and 2.75 mm thicknesses are unable to sustain the load and pressure, with the weakest area identified between the natural rubber and the metal cast iron that contacts the car's body. Overall, the research achieved its objectives, and the findings will be effectively applied to model the extended handle pneumatic floor jack, facilitating tire lifting for maintenance and tire changes.

1. Introduction

While changing a tire or performing other repairs on an automobile, it is sometimes necessary to lift the entire vehicle, depending on the situation from the ground. Various jack types have been developed for this purpose, but traditional manual jacks require a significant amount of skill and effort from the user and are heavy, large, and difficult to carry or position beneath an automobile. Additionally, large, adequate-position car lifting is frequently found in commercial and maintenance centers' service stations [1]. Additionally, railroads, pipeline shifting, and aircraft building and maintenance all employ it. Younger drivers, women, and elderly drivers who are physically weaker than average may find it extremely difficult to conventionally jack a car [2].

The airbag can withstand the shearing force and is made to be employed in certain lever-type applications. The three virtual procedures that are required for efficient working and traveling are reconditioning, mending, and replacing; persistent fatigue may even cause the tires to rupture [3]. And the pneumatic jack serves an excellent and vital duty in fixing this issue so that the vehicle can keep moving forward. Light vehicles only utilize a manual pneumatic jack, which is difficult to use and requires manual impact power, while almost all four-wheelers have a pneumatic jack for maintenance and reconditioning [3].

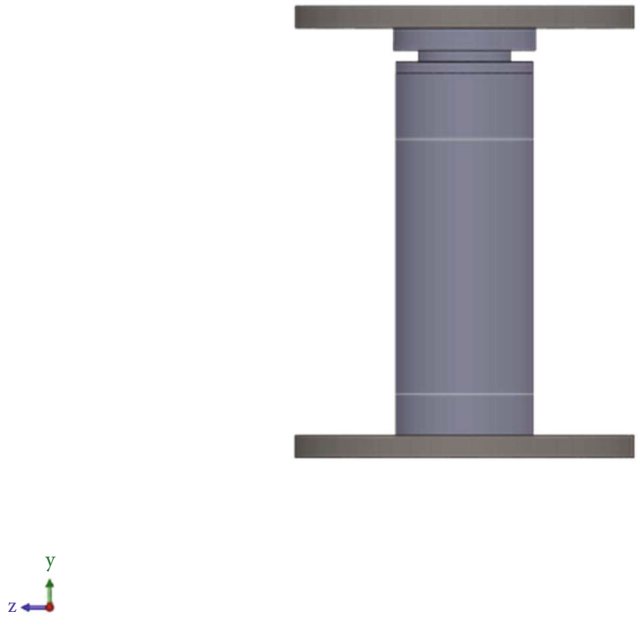

Figure 1: Telescopic shaft at idle position.

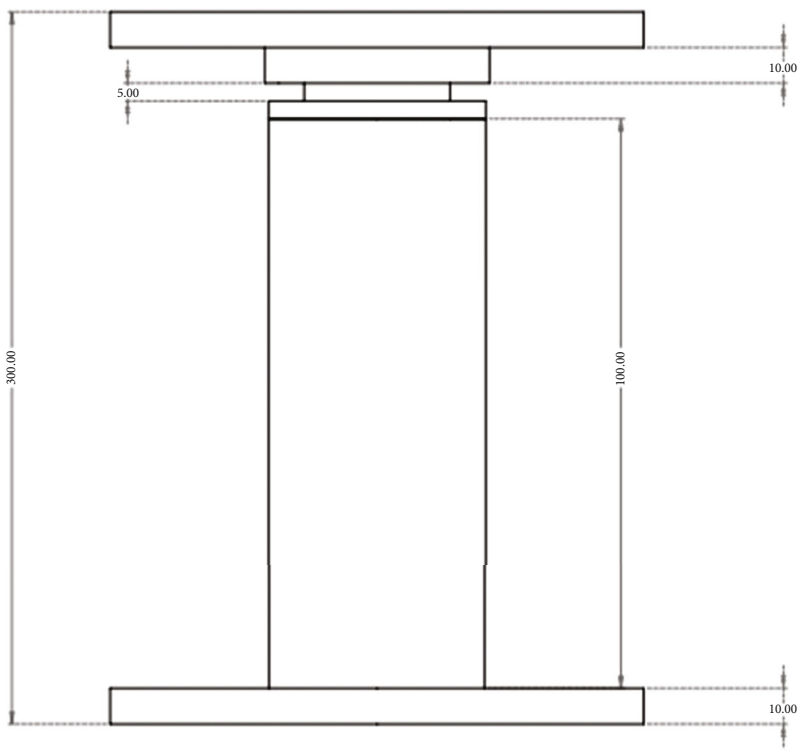

Figure 2: Telescopic shaft dimension at idle position.

Table 1: Dimensions of the telescopic shaft (mm) at idle position.

No.	Telescopic outer diameter (d) (mm)	Telescopic inner diameter (d_1) (mm)	Telescopic height (h) (mm)	Telescopic total height (h_t) (mm)	Telescopic base diameter (d) (mm)	Telescopic head diameter (d_2) (mm)
1	60.86	40.86	160	200	150	63

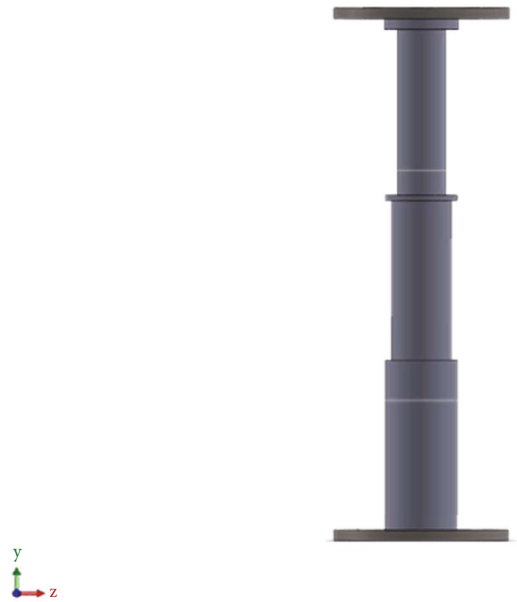

Figure 3: Telescopic shaft 3D model at extended position.

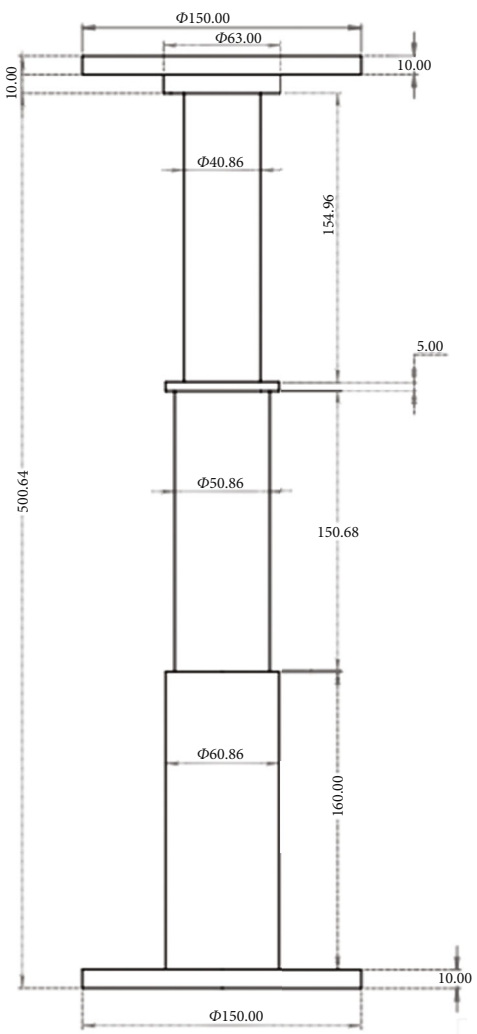

Figure 4: Telescopic shaft 3D dimensions at extended position.

Table 2: Dimensions of the extended telescopic shaft.

No.	Telescopic diameter (mm)	Telescopic height (mm)	Total height of telescopic (mm)	Telescopic base diameter (mm)	Telescopic head diameter (mm)
1	40.86	164.96			
2	50.86	155.68	500.64	150	63
3	60.86	160			

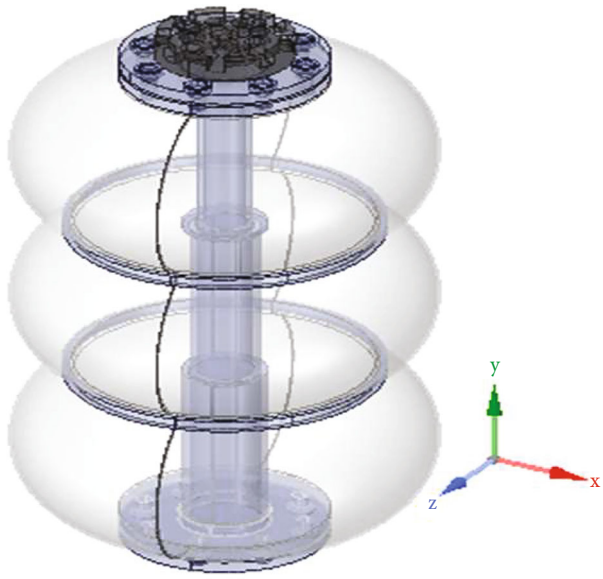

Figure 5: The preview of the designed pneumatic floor jack.

Pneumatic force is used by stronger jacks to elevate more things over greater distances. Pneumatic jacks consume regular power and have the potential to suddenly dislocate from their installation place, whereas mechanical jacks are frequently approved for maximum lifting capacity [4]. The primary limitations of a mechanical hydraulic jack's design are that it requires manual impact force to operate, consumes time and energy, and can be challenging for a worker in a garage. Taking into account each of these drawbacks, the quick-lifting hydraulic jack was developed. When it comes to maintaining and replacing tires, light-duty cars use a traditional mechanical jack as part of their equipment. Because the impact power is necessary, as was previously said, the pneumatic jack with gear arrangement is made affordably to manage these challenges [4]. Senior adults will most benefit from this since it offers a straightforward, safe automated pneumatic jacking mechanism that requires no physical labor, to offer a unique jacking mechanism that is controlled by a valve control from within the car. There are currently certain devices that can be used to lift the car wheels for the same reason [4].

Pneumatics, the study and use of pressured air to create mechanical motion, is the foundation of fabrication. Installing a pneumatic jack in a four-wheel drive vehicle can alleviate issues that may arise with traditional hydraulic jacks. This model is manufactured and includes a tiny reciprocating air compressor powered by a battery for four-wheelers, an air tank to hold compressed air, a pneumatic control valve to control airflow, and a double-acting cylinder that doubles as a jack for lifting tasks [5]. As a result, the car is raised using a jack, and tire-related issues including flat tires, tire replacement, and wheel balancing may be fixed quickly and easily. When operating a four-wheel drive vehicle and encountering a tire issue, a laborious manual process is employed to elevate the vehicle. This involves using a hydraulic or manual jack that requires additional human labor and time. Harmful impacts, such as thermal shock loads [6], can be effectively mitigated by appropriately implementing a pneumatic jack. The process involves positioning the jack in a stable position and then exerting force to screw it in, creating a spherical and transitional motion that raises the vehicle. We suggest creating a manufactured model based on pneumatics to save time and effort [5].

When the integrated pneumatic car jack with compressed air operation is made available for vehicles, it will be a widely sought-after jack. It is quite helpful for elderly folks and pregnant women. It minimizes human labor and is used for corporate purposes [7].

When changing tires, drivers need a lifting device jack that fits into a slot that is strategically placed beneath the vehicle. To facilitate and expedite the process of maintaining and replacing parts, pneumatic jacks are an essential tool in workshops and maintenance facilities. The current jacks at maintenance shops are heavy for women and the elderly to lift, and they are particularly inconvenient during inclement weather. However, the proposed machine solves these

Table 3: Specification of Land Cruiser 79 and Hilux double cabin pickup.

Item no.	Parameter	Detail description	
		Land Cruiser 79	Hilux double cabin
1	Model code	HZJ79-DKMRS	LAN25L-PRMDEN
2	Drive	4 × 4	4 × 4
3	Transmission	5-speed and manual	5-speed and manual
4	Suspension	Front: coil and rear: leaf	Front: double triangle and rear: rigid axle with leaf spring
5	Brakes	Front: disc and rear: drum	Front: disc and rear: drum
6	Number of doors	4	4
7	Number of seats	6	6
8	Seat material	Vinyl	Vinyl
9	Engine model	1HZ	5L-E
10	Color	White, silver metallic, grey, blue	White, grey, black, blue
11	Displacement (mm)	4164	2986
12	Number of cylinders	6	4
13	Maximum power (km/rpm)	96/3800	70/4000
14	Maximum power (bhp/rpm)	129/3800	94/4000
15	Maximum torque (Nm/rpm)	285/2200	197/220
16	Electrics (volts)	12	12
17	Fuel type	Diesel	Diesel
18	Fuel tank capacity (liters)	130	80
19	Curb weight (kg)	2280	1870
20	Gross vehicle weight (kg)	3200	2710
21	Payload (kg)	920	840
22	Dimensions (mm)	$L \times W \times H$: 5240 × 1800 × 1980	$L \times W \times H$: 5255 × 1760 × 1810
23	Wheelbase (mm)	3180	3085
24	Ground clearance (mm)	235	265
25	Tires	Front and rear: 7.50R16-8 5.50F-Tubed	205R16
26	Tire type	Radial	Radial
27	Front and rear seating arrangement	1 + 2 and 3 forward facing	1 and 3 forward facing
28	Front and rear seating type	Bench	High adjustable and 3 seats (40/60)
29	Owner's manual English	Tool kit and jack	Tool kit and jack
30	Air conditioning	Light reminder warning with buzzer	Manual

problems and also utilizes an abundant renewable energy source, namely, air [8, 9]. The introduction of pneumatic floor jacks can increase productivity, minimize the skilled labor force, save time and money, and provide space for industrial, maintenance, and construction applications. To solve the problem in this regard, an extended-handle pneumatic floor jack plays an important role. The significance of this study is that it is simple to use for women, the elderly, or anybody who has a problem with their vehicle's tires in the shop and on the road by using a shop truck for maintenance purposes. More than two pneumatic floor jacks can be used in the maintenance center, but even a well-organized shop may not be able to use one or two four-wheeler jacks at a time. A pneumatic floor jack needs less space than a cylindrical pneumatic car jack and lifts the vehicle wheel at the desired height.

A few research works have extensively investigated the performance of pneumatic floor jacks. However, to the best of our knowledge, only one study has examined the impact of different airbag thicknesses on the jack's performance [1]. Unfortunately, this study did not consider the inclusion of an extended handle, which is crucial for protecting the end user from accidents and injuries in case of pneumatic bag issues.

In this paper, we propose a detailed pneumatic jack design that incorporates three valves: an air inlet valve, an air exit valve, and a relief valve. Additionally, to enhance user-friendliness and convenience, a high-strength steel extended handle has been implemented. Various parameters such as equivalent stress, total deformation, directional deformation, and principal elasticity strain to ensure the effectiveness of the extended handle are evaluated. The design of the jack also takes into consideration the necessary capacity, dimensions, and lifting speed requirements to optimize its performance. The findings will be effectively applied to model the extended handle pneumatic floor jack, facilitating tire lifting for maintenance and tire changes.

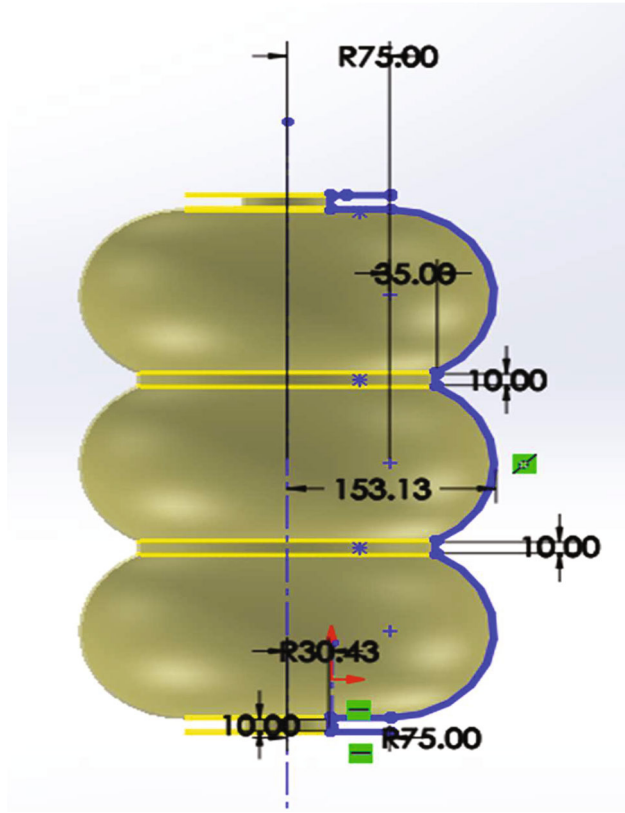

Figure 6: Pneumatic floor jack dimensions.

Table 4: Summary of the dynamic analysis of frequencies of telescopic shaft and airbag applied on six different deformation forces.

No.	Frequency values (Hz)	f_1	f_2	f_3	f_4	f_5	f_6
1	Telescopic	160.79	643.12	1447.03	2572.49	4019.52	5788.11
2	Airbag	323.43	1293.85	2910.5	5174.22	8084.72	11642

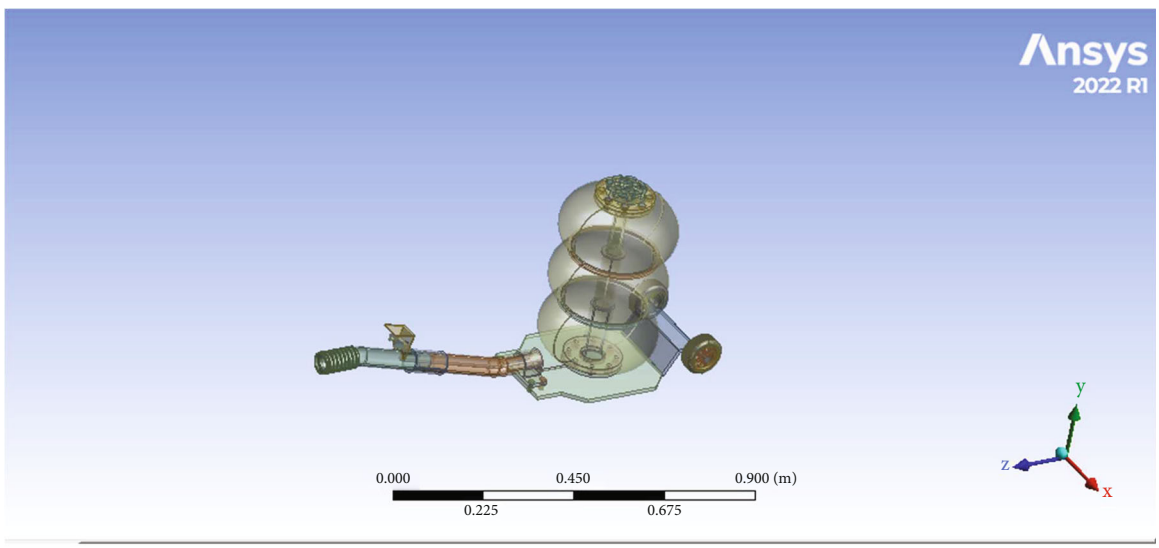

Figure 7: The 3D model of the pneumatic bag floor jack.

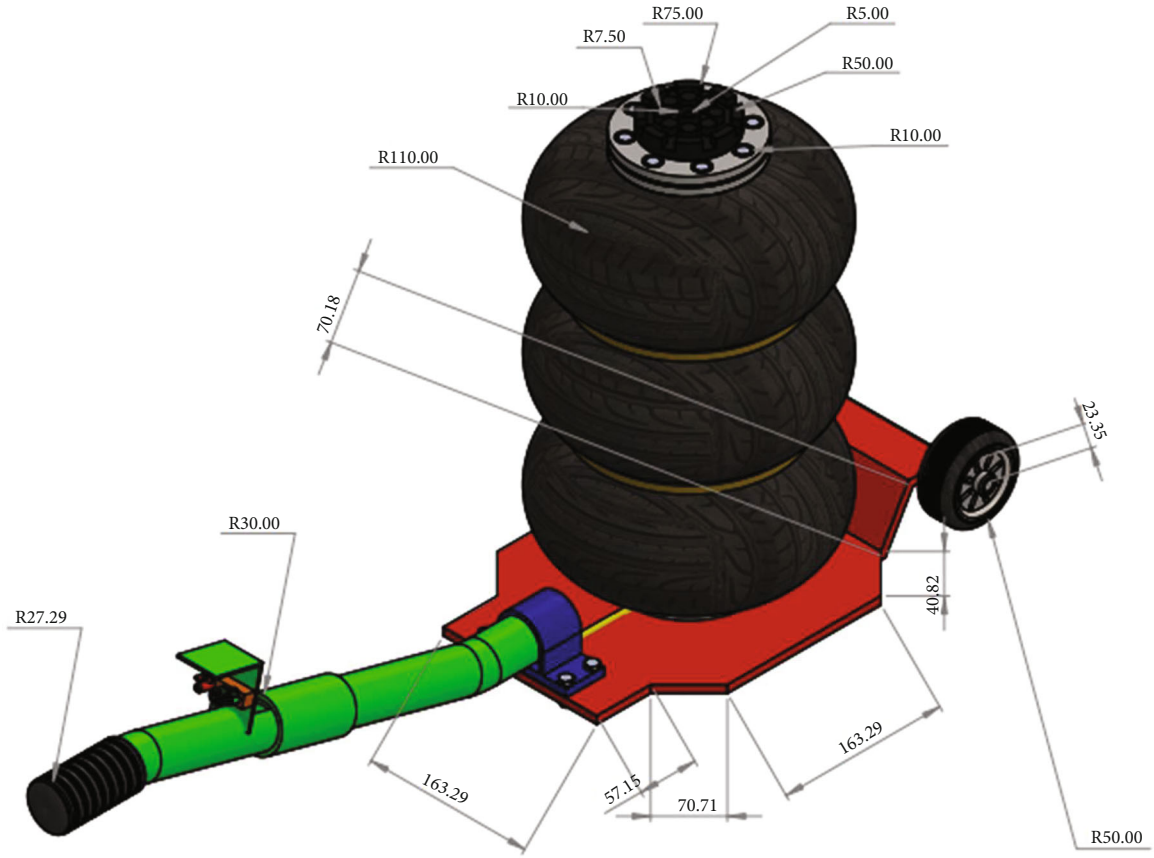

Figure 8: The 3D models of a pressurized pneumatic bag jack.

Table 5: Isotropic elasticity engineering data of the structural steel, stainless steel, and tire rubber.

No.	Properties	Structural steel value	Stainless steel values	Tire rubber value
1	Density (kg/m^3)	7850	7750	1000
2	Young's modulus (MPa)	2.00*E*+11	1.93*E*+11	1.00*E*+06
3	Poisson's ratio	0.3	0.31	0.3
4	Bulk modulus (MPa)	1.67*E*+05	1.69*E*+05	8.33*E*+05
5	Shear modulus (MPa)	7.69*E*+04	7.37*E*+04	3.85*E*+05
6	Tensile yield strength (MPa)	250	205	22
7	Compressive yield strength (MPa)	250	205	22
8	Tensile ultimate strength (MPa)	460	586	5
9	Compressive ultimate strength (MPa)	0	0	0
10	Structural steel coefficient of thermal expansion (1/°C)	1.20*E*-05	1.70*E*-05	

2. Methodology

2.1. Design of Telescopic Shaft at Idle and Extended Position. When the pneumatic jack is at an idle position, there is no air accumulated in the airbag and the telescopic shaft at the bottom level. The cross-sectional areas of the telescopic shaft are calculated using

$$A = \frac{1}{4}\pi(d - d_i)^2, i = 1, 2, 3 \cdots, \quad (1)$$

where A is an area of cross-section, d is the external diameter of the shaft, and d_i is the internal diameter of the shaft.

Figure 1 shows the telescopic shaft at an idle position, while the telescopic shaft's detailed dimensions are originated in Figure 2 and Table 1.

Figure 3 shows the telescopic shaft at an extended position, while the telescopic extended shaft's detailed dimensions are described in Figure 4 and Table 2.

Most compressed air equipment is designed to operate at around 6-10 bar (500-1000 kPa) (http://www.air-compressor-guide.com). So the capacity of the compressor at the Ethiopian

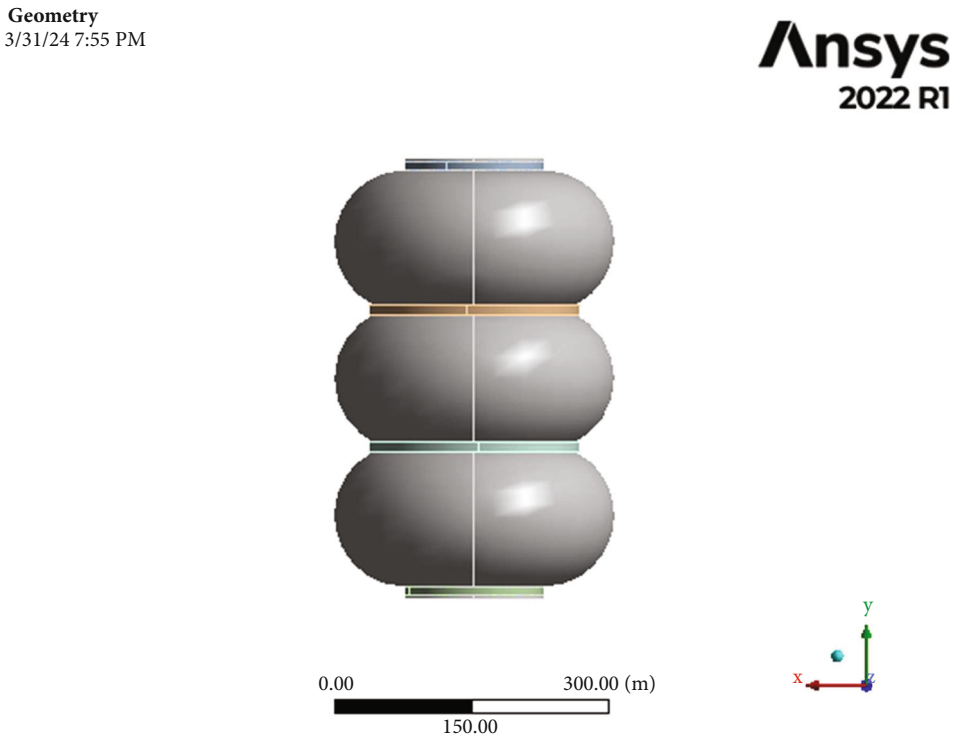

Figure 9: The imported 3D model tire rubber.

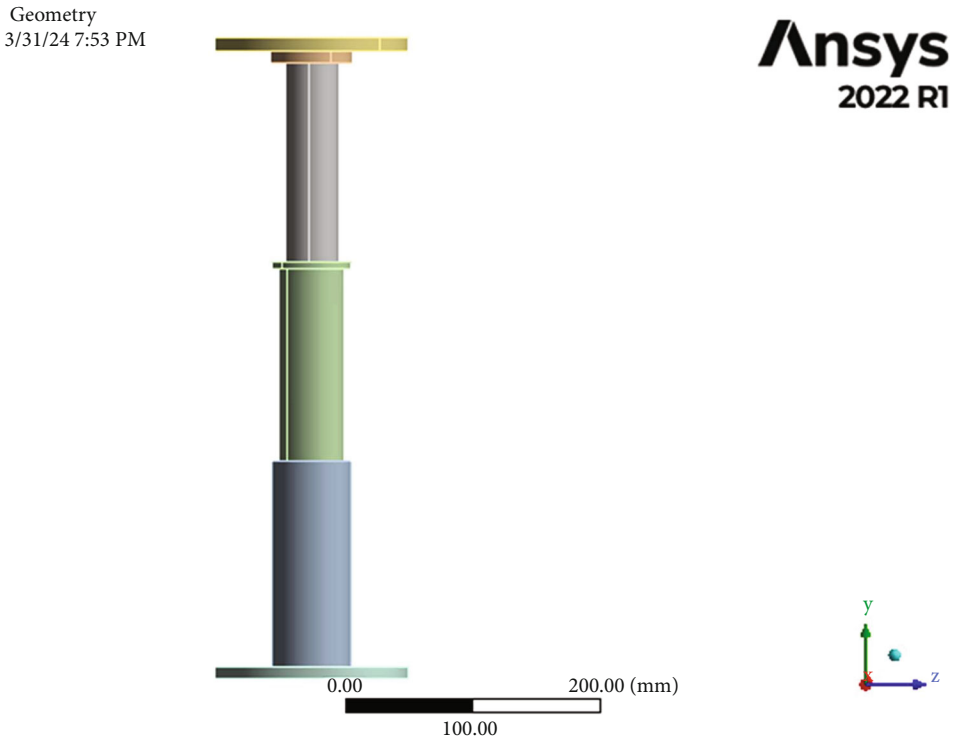

Figure 10: The imported 3D model telescopic shaft.

Construction Works Corporation Maintenance Center (ECWCMC) is 8.5 bar (850 kPa) which is taken as the reference.

2.2. Design of Pressurized Pneumatic Bag. Figure 5 shows the preview of the designed pneumatic floor jack. Toyota Pickup Vehicle is selected for pneumatic jack design, and analysis of

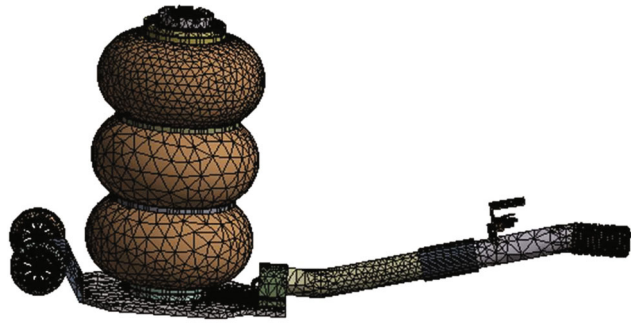

Figure 11: Meshed model of extended handle pneumatic bag floor jack.

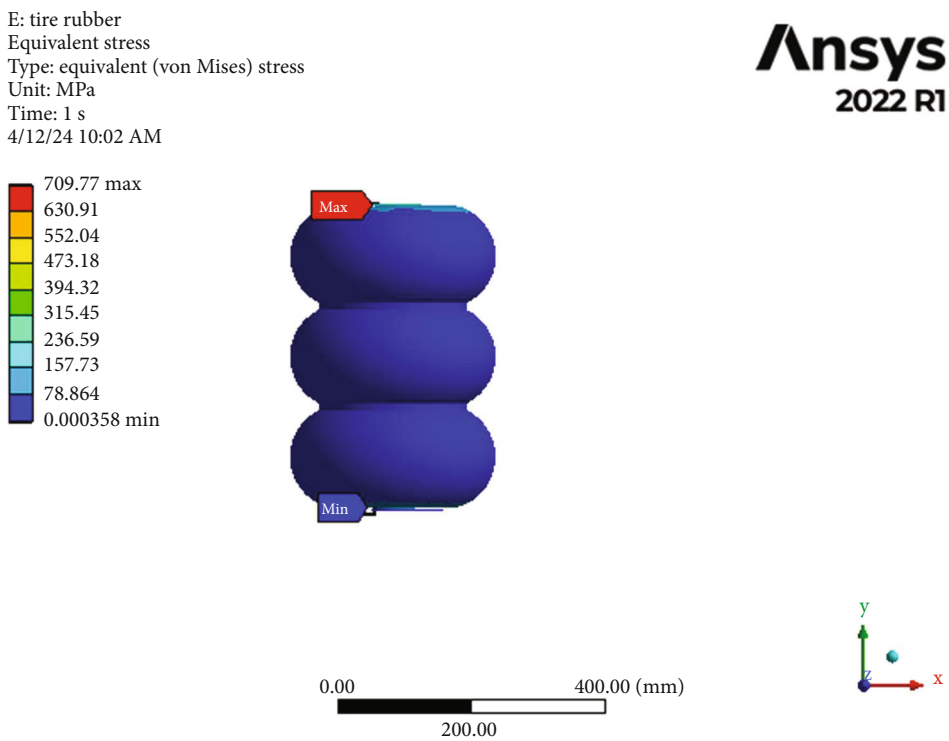

Figure 12: Equivalent (von Mises) stress of airbag at 2.5 mm thickness.

the specification of the Toyota Land Cruiser 79 and Hilux double cabin is given in Table 3.

To determine the areas of the pneumatic bag jack shown in Figure 6, the cylindrical area calculation is used as shown in

$$A_T = 2\pi r^2 + h(2\pi r), \tag{2}$$

where A_T is the total area of the airbag, r is the radius, and h is the height.

According to the specifications in Table 4, the vehicle's curb weight includes the weight of all standard equipment and a full fuel tank. Any additional equipment, passengers, or cargo weight is not included in the weight. The weight at the curb is said to be the closest measurement to the car's actual weight. Pressure is force per unit area (equation (3)); the expression for force in terms of mass can be used to solve pressure as well, which can be expressed as

$$P = \frac{F}{A} = \frac{\text{mg}}{A}. \tag{3}$$

In equation (3), P represents the pressure exerted on the system, F indicates the force applied on the telescopic shaft, and A is the cross-section area load applied to the telescopic shaft.

Weighing a vehicle on a big scale allows for the precise determination of its real weight. Truck stops and locations, where goods are loaded onto trucks, are common places to find scales for vehicles and trucks.

The vehicle payload or passenger/cargo capacity can be subtracted from the gross vehicle weight rating (GVWR) to determine the curb weight. The GVWR is shown on the door jamb label, or compliance label, of the vehicle. It is possible to find the payload or passenger/cargo weight capacity on the tire specification label that is situated in the door jamb area.

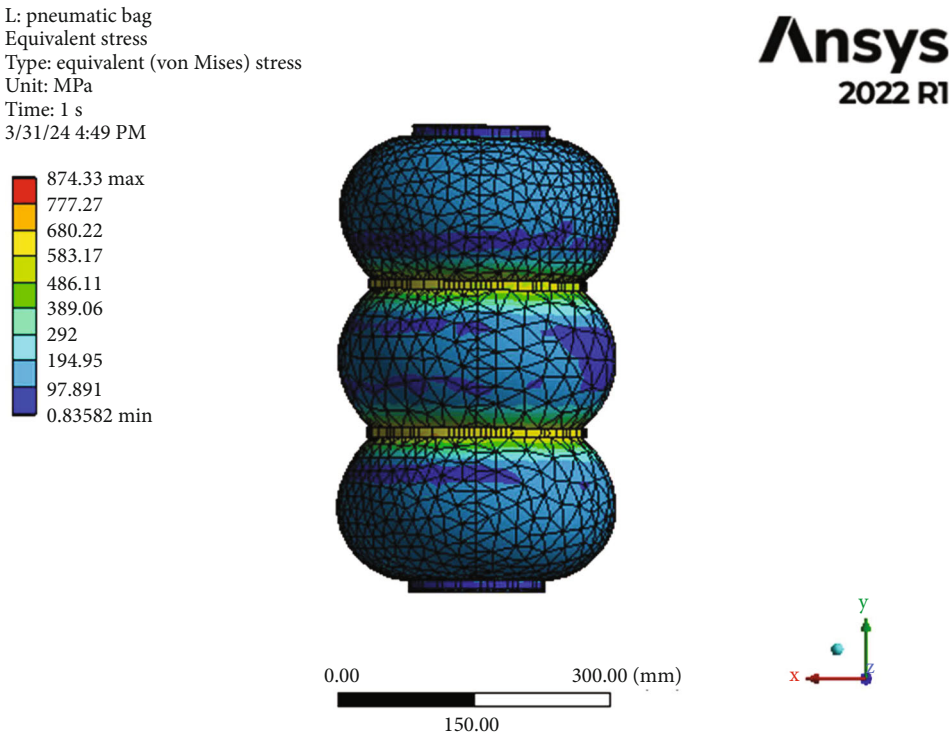

Figure 13: Equivalent (von Mises) stress of airbag at 2.75 mm thickness.

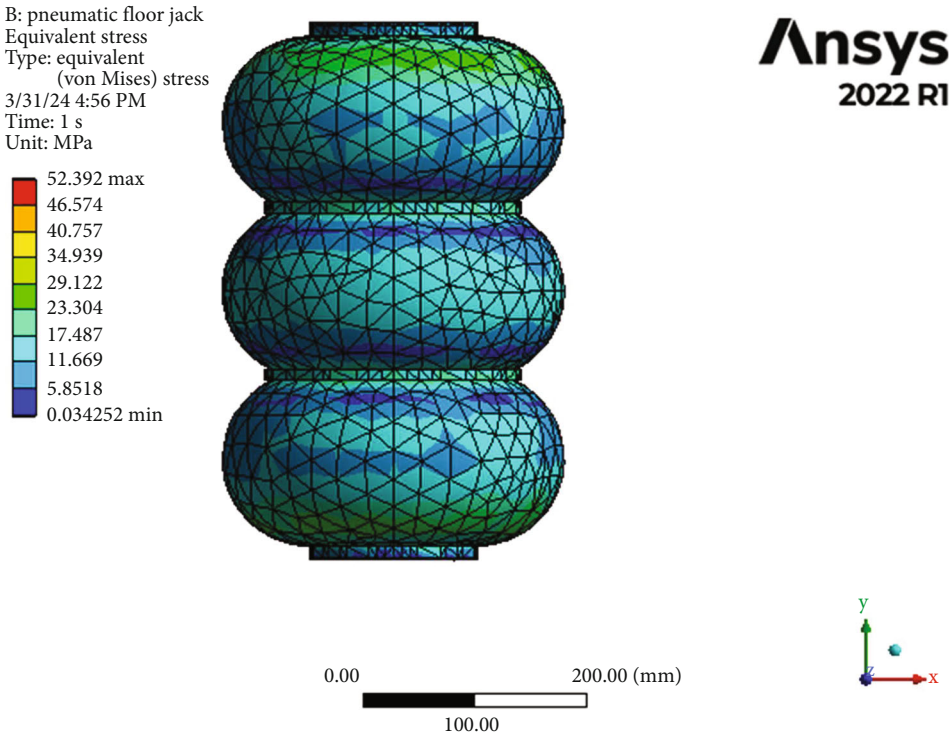

Figure 14: Equivalent (von Mises) stress of airbag at 3 mm thicknesses.

From Table 4, two large-weight vehicles (Toyota Land Cruiser HZJ79L and Toyota Hilux double cabin pickup) were selected as a sample to calculate the load of the payload of the vehicle = 950 kg and 840 kg, respectively.

The curb weight of both vehicles is 2280 kg and 1870 kg, respectively.

The calculated total masses of the vehicles are the sum of payload + curb weight = 3200 kg and 2710 kg and take acceleration due to gravity $(g) = 9.81\ \text{m/s}^2$.

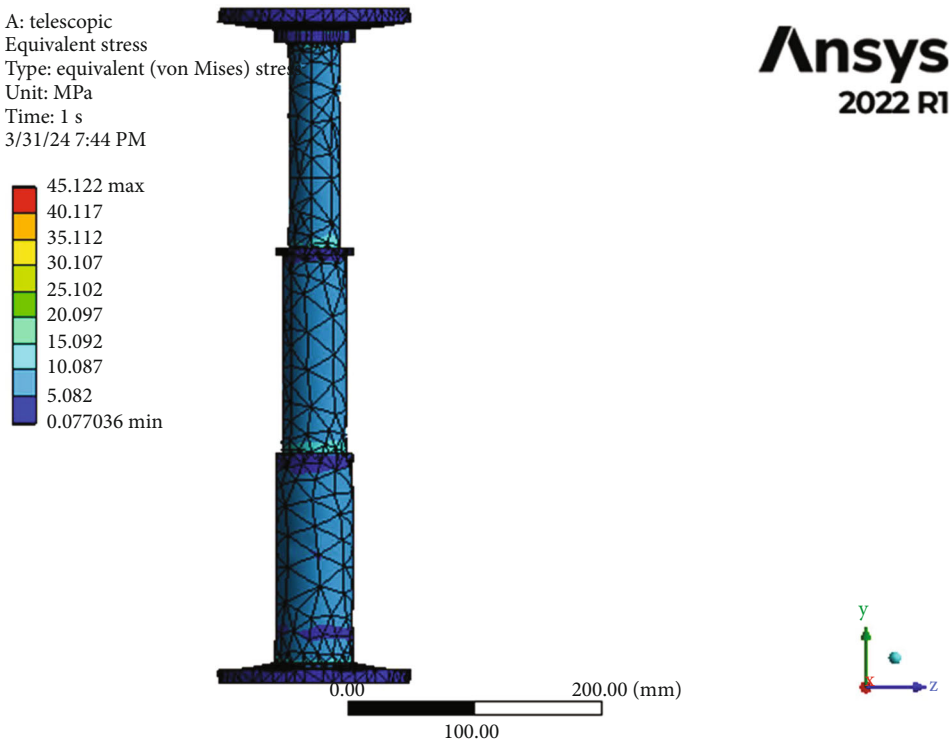

Figure 15: Equivalent (von Mises) stress of telescopic shaft.

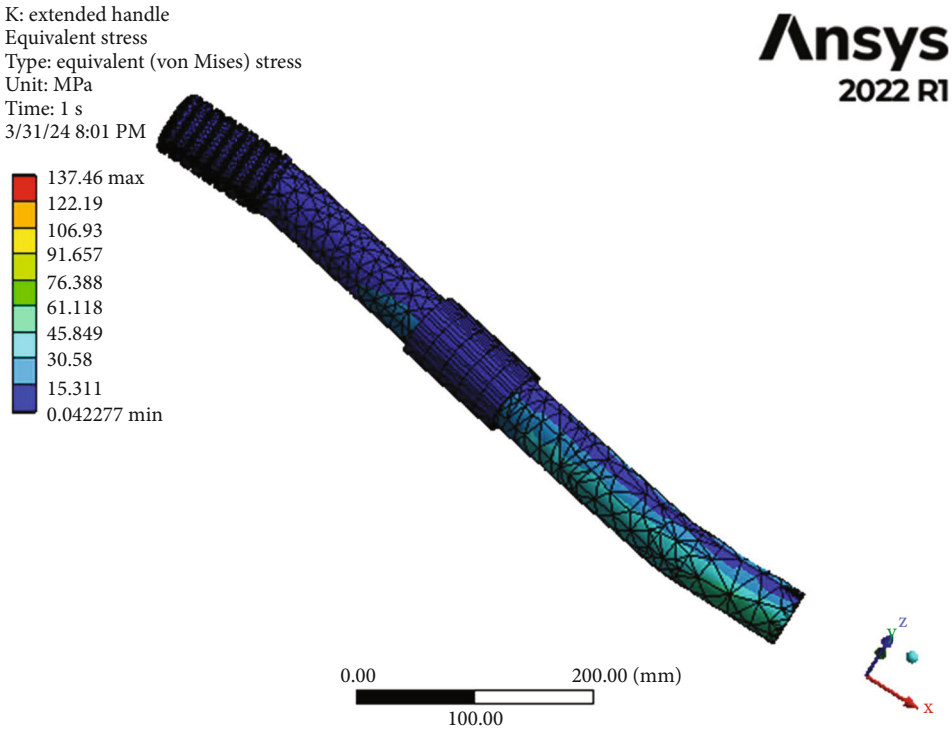

Figure 16: Equivalent (von Mises) stress of extended handle.

The value of factor of safety [10], ranges from 1.3 to 2.25 and then takes a factor of safety of 1.5.

Therefore, let us take the large weight to calculate a total weight $(W_T) = 3200\,\text{kg} \times 10\,\text{m/s}^2 \times 1.5 = 48{,}000\,\text{N}$.

Because the vehicle has four wheels, a pneumatic jack lifts one wheel from the ground at a time. So, the weight of one wheel is one-fourth of the total weight which is 8000 N.

Table 6: Summary of the results of static structure pneumatic Jack.

Comparisons of jacks	Max. equivalent stress (MPa)	Max. allowable stress (MPa)	Max. total deformation (mm)	Max. principal deformation (mm)	Equivalent elastic strain (mm/mm)
Telescopic shaft	45.12	608.65	2.97*E*-02	1.88*E*-03	2.55*E*-04
Pneumatic bag $T = 3$ mm	52.39	608.65	2.40*E*-07	3.39*E*-10	1.77*E*-10
Pneumatic bag $T = 2.75$ mm	709.77	608.65	1.98	0.08	3.79*E*-03
Pneumatic bag $T = 2.5$ mm	874.33	608.65	3.36	0.41	4.49*E*-03

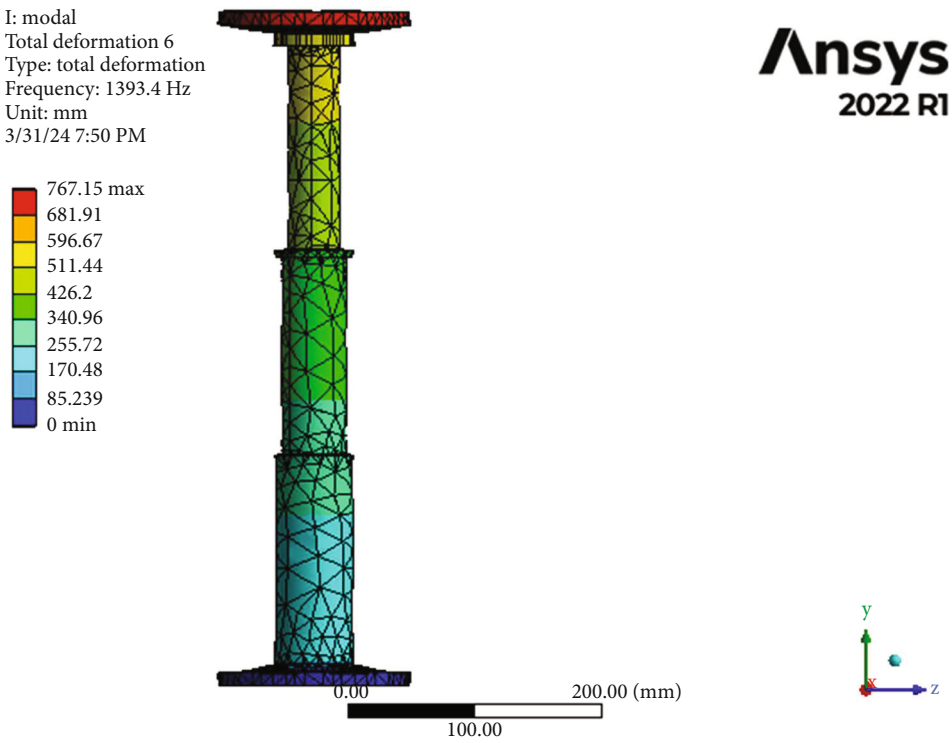

Figure 17: Total deformation of the telescopic shaft at frequency 1393.4.

2.3. Analysis of Pneumatic Bag Jack Using FEM. Systems that are too complex to manually evaluate are usually built and optimized using this kind of study. Systems that fall into this category have governing equations, scales, or geometry that are too complicated [11].

A static structural analysis determines the displacements, strains, stresses, and forces brought about by loads on structures or components that do not significantly affect their damping effects or moment of inertia. The loads and the structure's response are assumed to be stable throughout time, meaning that there will be only slight variations in both. A static structural load can be computed using the ANSYS solver [12]. You can utilize the following loading types in a static analysis:

(i) Externally exerted pressures and forces

(ii) Inertial forces in a steady state, such as rotational velocity or gravity

(iii) Imposed (nonzero) displacements

(iv) Temperatures (to thermal strain)

These features make use of more static loading conditions that remain constant in terms of place and time.

(i) The load applied on the pad of the pneumatic bag jack is considered a part of the jack

(ii) The telescopic shaft automatically actuated when the compressed air was supplied to the pneumatic bag jack and the pressure was applied on the whole geometry of the pneumatic bag as shown in Figure 7. Figure 8 also shows the dimensions of a 3D model of the pneumatic bag jack

Structural steel is the material selected for designing the telescopic shaft, and the components of the pneumatic bag jack are the upper and lower plate, base plate, rings, handles, and grooved pad on the top of the bag.

2.4. Dynamic Analysis of Pneumatic Bag Jack. The appearance inspection and static and dynamic load tests of steel structure bridges are the keys to verifying their

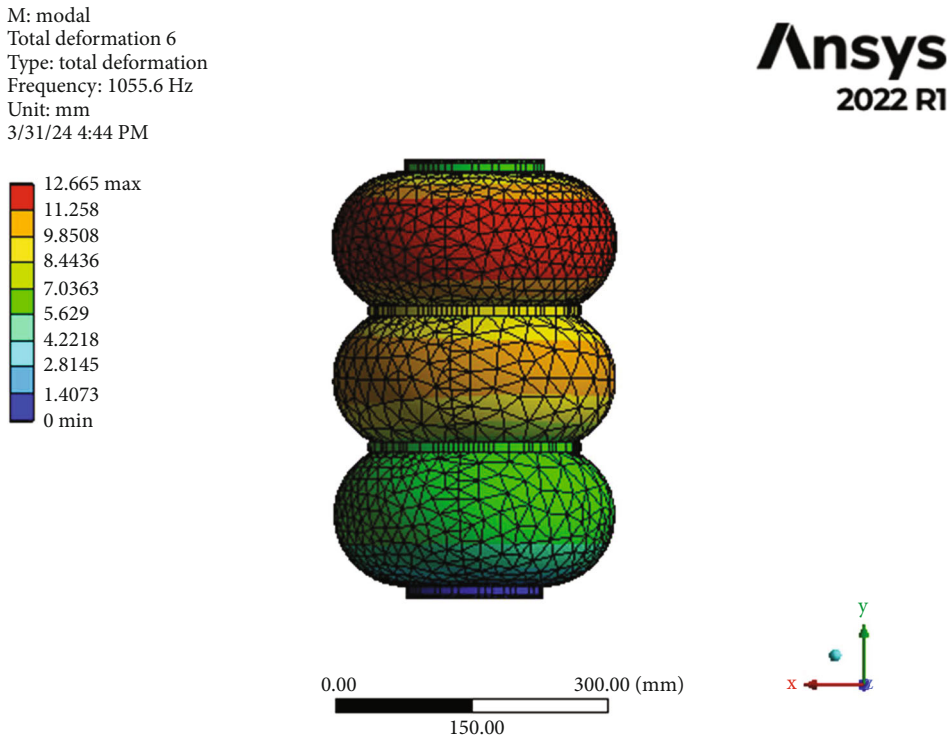

Figure 18: Total deformation of the airbag at 1055.6 Hz frequency.

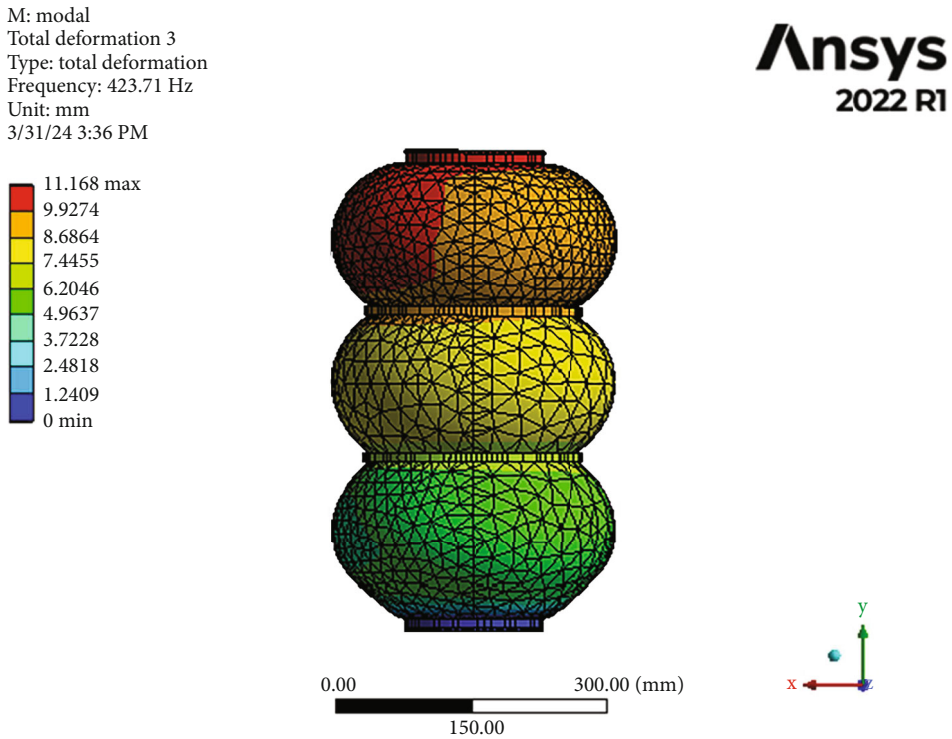

Figure 19: Total deformation of the airbag at 423.71 Hz frequency.

mechanical performance [13]. The Euler-Bernoulli beam theory of the transferring loads and deflection characteristics of beams was reviewed to calculate the natural frequency (f_n) of the telescopic shaft and pneumatic bag (equation (4)). The calculated values are tabulated in Table 4.

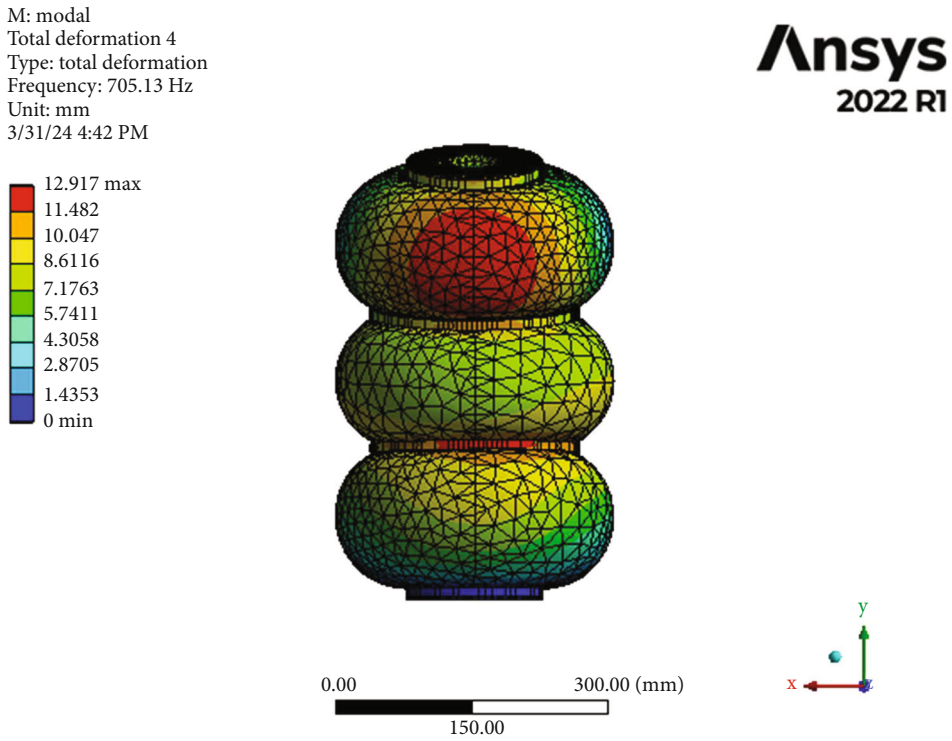

Figure 20: Total deformation of the airbag at 705.15 Hz frequency.

$$f_n = \frac{1}{2\pi}\left[\frac{n\pi}{L}\right]^2 \sqrt{\frac{EI}{\rho}}, n = 1, 2, 3 \cdots \cdots \cdots \ldots, \quad (4)$$

where n is the mode shape, L is the length of the telescopic shaft, E is the modulus of elasticity for stainless steel, I is the momentum of inertia, and ρ is the density of the material.

2.5. Static Analysis of Pneumatic Bag Jacks

2.5.1. Engineering Data. The properties of structural steel, stainless steel, and tire rubber are presented in Table 5.

2.6. Geometry. Provide multiple options to set the properties of the 3D model geometry to import from the compatible IGES file before attaching the geometry of the pneumatic bag jack rubber and telescopic shaft. The choices are as follows: CAD associativity, importing coordinate systems, importing work points, solid bodies, surface bodies, line bodies, parameters, attributes, named selections, and material properties are all exclusive to the design modeler application. Other features include saving updated CAD files in reader mode, "smart" refreshing of models with unmodified components, and allowing parts of mixed dimensions to be imported as assembly components that have parts of mixed dimension.

Figures 9 and 10 illustrate the geometry of the elongated pneumatic bag and telescopic shaft, respectively.

2.7. Mesh Generation. By applying mesh, contact surfaces are given a sufficient mesh density to enable the smooth distribution of contact stresses. The fundamental variables that need to be resolved are the total deformation, equivalent (von Mises) stress, strain, normal stress, and shear force. The solution output gives useful information on how the structure behaved during the analysis and continuously refreshes any listing that the solver produced. The quality of the mesh was assessed using mesh metrics, such as aspect

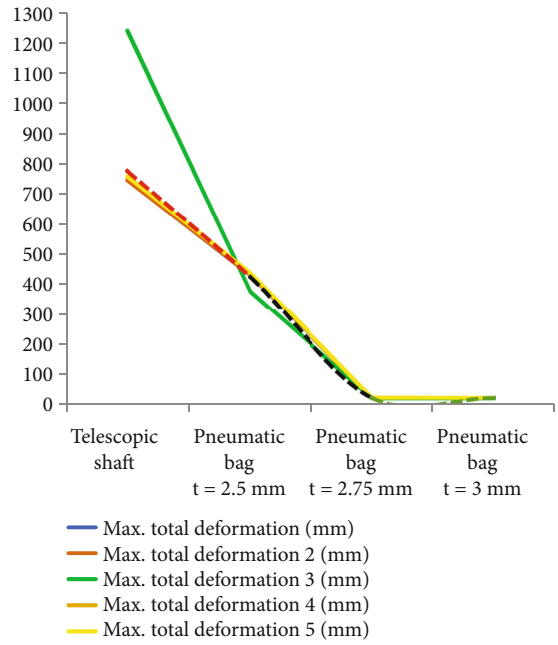

Figure 21: The comparison chart of the maximum total deformation of the pneumatic bag and telescopic shaft at different points.

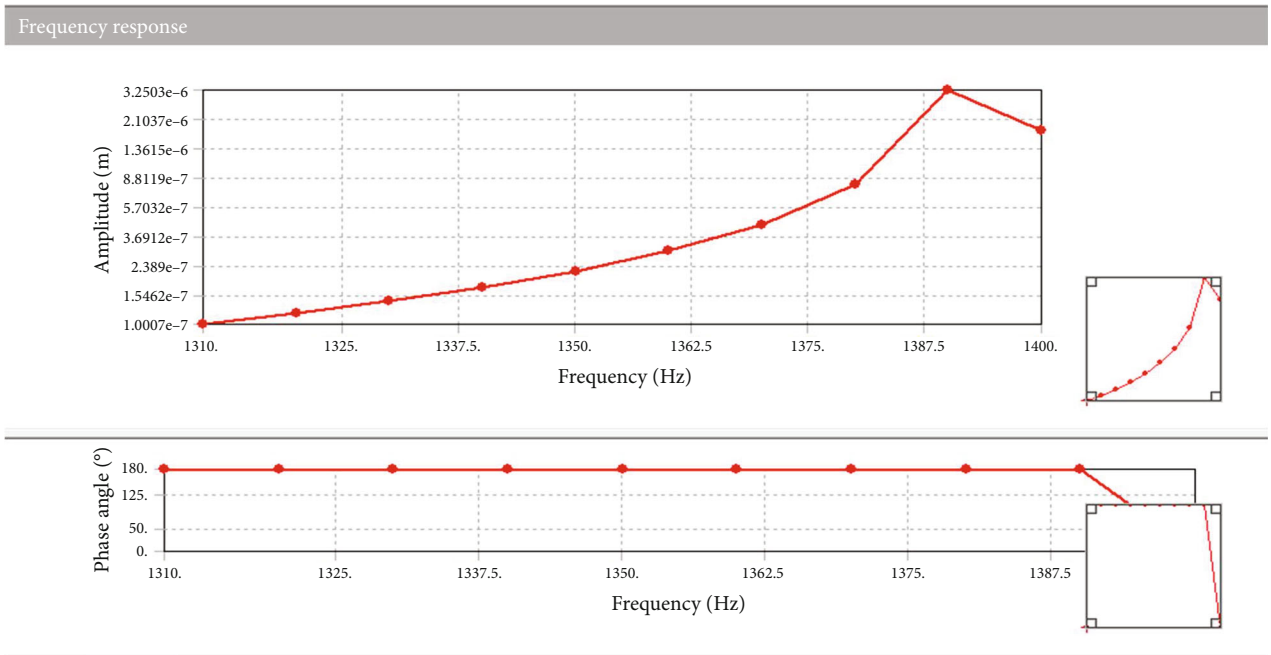

Figure 22: The deformation of telescopic frequency response.

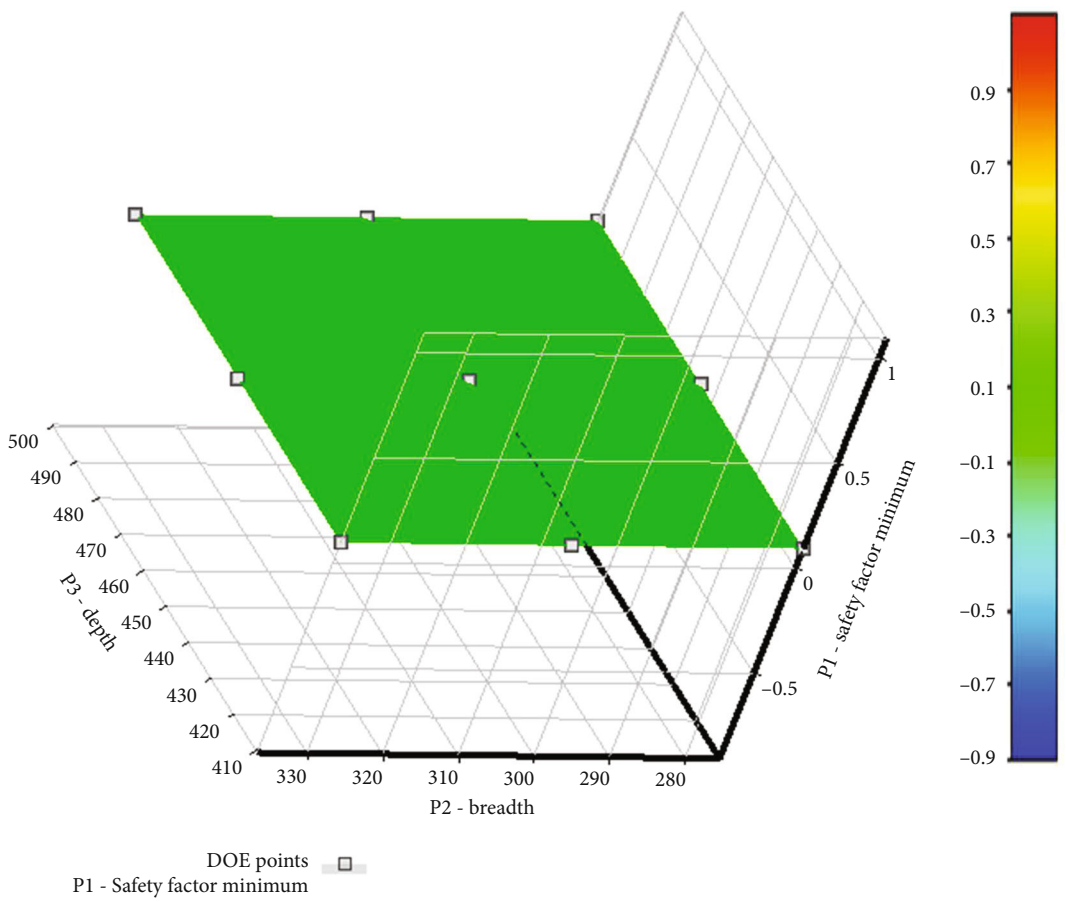

Figure 23: Response surface optimization charts for P1 safety factor minimum.

Table 7: Optimization candidate points.

Candidate points	Candidate point 1	Candidate point 2	Candidate point 3
P2-breadth	275.42	283.38	336.58
P3-depth	409.52	421.08	496.21
P1-safety factor minimum	0.095455	0.095455	0.095455

Table 8: Validation of the designed pneumatic jack.

Types of pneumatic jack	Weight lifting capacity	Mechanism
Design of pneumatic operated jack for four-wheelers	25 kg at pressure 3.27 bar	Four-wheeler
Design and development of integrated pneumatic car jack	25 kg at a pressure of 2 bar	Four-wheeler
Design and development of integrated pneumatic car jack	60 kg at pressure 5 bar	Cylindrical piston
Design and analysis of pneumatic bag air jack	1.25 ton at pressure 2.498 bar	Airbag jack
Design and analysis of extended handle pneumatic floor jack	3 tons at pressure 8.5 bar	Extended handle pneumatic jack

ratio, skewness, and orthogonal quality [14]. The meshed extended handle pneumatic bag floor jack is shown in Figure 11.

3. Result and Discussion

3.1. Static Structural Analysis. The pneumatic bag with thicknesses of 2.5 mm and 2.75 mm does not reach the intended design outcome. As shown in Figures 12–14, the values obtained are for the pneumatic bag 3 mm thickness.

The equivalent (von Mises) stress of the telescopic shaft and the equivalent (von Mises) stress of the extended handle are labeled in Figures 15 and 16, respectively.

The summary of the static structure of pneumatic jacks is calculated in Table 6.

3.2. Dynamic Analysis. The total deformation of the telescopic shaft and airbags at different frequencies are shown in Figures 17–20.

The result of the maximum total deformation of the telescopic shaft and pneumatic bag at different six points is summarized in Figure 21.

Table 6 shows the maximum total deformation at various points of the pneumatic bag, and this is further illustrated in the chart presented in Figure 22. It is evident that as the thickness increases, the deformation size decreases. Therefore, the optimized thickness is 3 mm.

3.2.1. Response Surface Optimization. A collection of statistical and mathematical tools called response surface methodology (RSM) is used in the creation of empirical models. The goal is to maximize an output variable (response) that is affected by multiple independent variables (input variables). Response surface optimization and direct optimization are two popular optimization techniques. The direct optimization approach uses the experimental design method to get several experimental design points. It then solves each experimental design point individually to determine the optimal solution, resulting in a huge calculation and low solution efficiency. Building explicit constraints or goal functions in the initial design issue is known as response surface optimization, and it significantly increases the optimization's efficiency [15]. The response surface optimization for the P1 safety factor minimum is discovered in Figure 23.

The process for optimization is to find all the candidate points and then to see which gives the highest and lowest values in Table 7.

3.2.2. Validation of the Result. The designed pneumatic jack was compared and validated with existing pneumatic jacks in terms of weight lifting capacity and lifting mechanism (Table 8).

4. Conclusions

Increasing the rubber thickness has a positive effect on the performance of the pneumatic floor jack.

The study applied 8.2 MPa of pressure and found that using a 2.5 mm thickness resulted in a maximum von Mises stress of 874.33 MPa while using a 3 mm thickness resulted in a stress level of 52.392 MPa, as shown in the table. The stress levels for the 2.5 mm and 2.75 mm thickness exceeded the acceptable stress by 44% and 16% (608.65 MPa), while the 3 mm thickness was 91% less than the allowable stress and could withstand the load. The 2.5 mm thickness exceeded 44% of this limit, while the 3 mm thickness was 92% less and could easily sustain the load. An increase in rubber thickness resulted in a decrease in total deformation, so the 3 mm airbag thickness jack exhibited significantly less deformation. Therefore, the optimum design among the three thicknesses is 3 mm thickness.

Future research endeavors will focus on advancing movable compressor technology to enable the widespread use of pneumatic bag jacks for light vehicles. Additionally, there is potential to explore the design of an inbuilt jack within the car body that utilizes the air source from exhaust gas.

Data Availability

Data will be made available on request.

Conflicts of Interest

The authors declare no conflict of interest.

Authors' Contributions

Abduljebar Mahmud, Ramesh Babu Nallamothu have significant contribution to the concept, analysis, and interpretation of the data and writing of the article. Abdulbasit Nasir critically drafted and revised the article for significant intellectual content and made a significant contribution to the concept of the article.

Acknowledgments

The authors extend their appreciation to Adama Science and Technology University for their cooperation and assistance during the study.

References

[1] T. C. Khidir, B. M. Qasim, and A. A. Abduljabbar, "Design and analysis of pneumatic bag air jack," *Journal of Mechanical Engineering Research & Developments (JMERD)*, vol. 42, pp. 61–63, 2019.

[2] R. N. Natarajan, "Machine design," *Handbook of Machinery Dynamics*, pp. 11–28, Eurasia Publishing House (Pvt.) Ltd., Ram Nagar, New Delhi-110 055, 1890.

[3] S. Chaudhry, H. Kolhe, S. Darzi, C. Hiwarkar, and M. Kharde, "Design and fabrication of pneumatic vice," *SSRN Electronic Journal*, vol. 25, pp. 603–605, 2022.

[4] P. D. Gawade, R. R. Gaikwad, A. M. Kakirde, and N. B. Gavhane, "Design and development of automatic pneumatic jack for four wheeler," *International Journal of Advance Research and Innovative Ideas in Education (IJARIIE)*, vol. 11, pp. 1721–1725, 2017.

[5] S. Gumphalwar, D. Dhabarde, S. Gade, A. Kalhane, V. Nair, and P. Randive, "Design and fabrication of pneumatic car lifter," *International Journal of Advance Research and Innovative Ideas in Education (IJARIIE)*, vol. 4, pp. 3435–3439, 2018, http://www.ijariie.com/.

[6] W. Xu, H. Han, Q. Li, M. Mollajafari, and F. Scott, "Layerwise formulation of poroelastic composite plate under pre-buckling and thermal shock loading," *Composite Structures*, vol. 304, article 116343, 2023.

[7] K. H. Pandya, A. V. Sawant, and V. S. Gurav, "Design and Development of Integrated Pneumatic Car Jack," *International Journal of Advanced Research in Science and Engineering*, vol. 7, no. 3, pp. 19–23, 2018.

[8] M. Negahban, M. V. Ardalani, M. Mollajafari, E. Akbari, M. Talebi, and E. Pouresmaeil, "A novel control strategy based on an adaptive fuzzy model predictive control for frequency regulation of a microgrid with uncertain and time-varying parameters," *IEEE Access*, vol. 10, pp. 57514–57524, 2022.

[9] A. Abdullah and A. A. Alzahrani, "Modeling and parametric analysis of a large-scale solar-based absorption cooling system," *Modelling and Simulation in Engineering*, vol. 2024, Article ID 6626705, 21 pages, 2024.

[10] D. V. Ramanareddy, B. Subbaratnam, E. M. Kumar, and P. K. Praneeth, "Design and analysis of composite leaf spring," *International Journal of Mechanical Engineering and Technology (IJMET)*, vol. 8, pp. 494–500, 2017.

[11] N. H. Beidokhti, M. Khoshgoftar, A. Sprengers, T. Van den Boogaard, D. Janssen, and N. Verdonschot, "A comparison between dynamic implicit and explicit finite element simulations of native knee joint," *Japanese Journal of Radiological Technology*, vol. 3, 2015.

[12] Z. Zhou, Y. Li, X. Chen, X. Shang, K. Gou, and L. Pang, "Optimization of the gas flow system in a selective laser melting chamber using numerical methods," *Advances in Mechanical Engineering*, vol. 16, no. 3, pp. 1–10, 2024.

[13] Y. Li, X. Luo, and Y. Li, "Experimental analysis of static and dynamic performance for continuous Warren truss steel railway bridge in heavy haul railway," *Modelling and Simulation in Engineering*, vol. 2024, Article ID 3767759, 15 pages, 2024.

[14] A. Nasir, E. Dribssa, M. Girma, and H. B. Madessa, "Selection and performance prediction of a pump as a turbine for power generation applications," *Energies*, vol. 16, no. 13, p. 5036, 2023.

[15] J. Xiangjie, Z. Cai, and W. Chong, "Response surface optimization of machine tool column based on ANSYS workbench," *Academic Journal of Manufacturing Engineering*, vol. 18, pp. 162–170, 2020.